THE JOURNAL OF PHYSICAL CHEMISTRY LETTERS
A JOURNAL OF THE AMERICAN CHEMICAL SOCIETY

pubs.acs.org/JPCL Letter

Indirect Detection of the Protons in and around Biradicals and their Mechanistic Role in MAS-DNP

Satyaki Chatterjee, Faith J. Scott, Snorri Th. Sigurdsson, Amrit Venkatesh, and Frédéric Mentink-Vigier*

Cite This: *J. Phys. Chem. Lett.* 2025, 16, 635−641 Read Online

ACCESS | Metrics & More | Article Recommendations | Supporting Information

ABSTRACT: The contribution of protons in or near biradical polarizing agents in Dynamic Nuclear Polarization (DNP) has recently been under scrutiny. Results from selective deuteration and simulations have previously suggested that the role of protons in the biradical molecule depends on the strength of the electron−electron coupling. Here we use the cross effect DNP mechanism to identify and acquire ^{1}H solid-state NMR spectra of the protons that contribute to propagation of the hyperpolarization, via an experimental approach dubbed Nuclear−Nuclear Double Resonance (NUDOR).

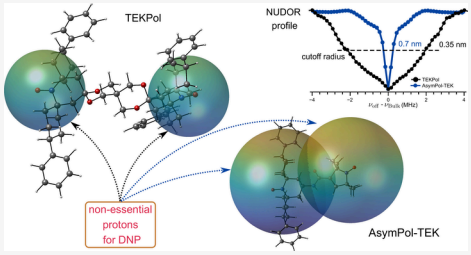

The weak coupling between nuclear spins and the magnetic field in Nuclear Magnetic Resonance (NMR) spectroscopy generates low nuclear spin polarization, which results in low signal-to-noise ratios and long signal acquisition times.[1,2] Dynamic Nuclear Polarization (DNP) uses the strong coupling of unpaired electron spins with the magnetic field to increase the sensitivity of solid-state NMR, with numerous reported applications in material science and biology.[3−8] A combination of Magic Angle Spinning (MAS) and DNP has been shown to yield high resolution and sensitivity in solid-state NMR.[2−6]

The unpaired electrons, that are often provided by biradical polarizing agents,[2,9,10] are typically used to hyperpolarize protons (^{1}H) using the cross effect (CE) mechanism under MAS.[11−18] Briefly, in CE DNP, the nuclear spins that are close to the biradical are hyperpolarized due to the presence of electron−nuclear hyperfine interactions, and ^{1}H−^{1}H homonuclear spin diffusion equilibrates this hyperpolarization with protons that are further away.

The protons in the biradicals have strong hyperfine couplings to the electron spins, which contains both isotropic and anisotropic components on the order of several MHz (see Figure S6). This coupling renders the spectra of such protons very broad and below the detection limit.[19,20] The hyperfine couplings modify the Larmor frequency and thus impacts the propagation of the spin hyperpolarization; this correlation is at the center of the concept called "spin diffusion barrier".[19−22] The situation is similar to heteronuclear spin diffusion,[23−26] and the importance of this "spin diffusion barrier" for MAS-DNP has been debated.[20,27,28] However, large spin system simulations have indicated that quantitative results can be obtained only if the protons in the biradical are considered,[25,26,29,30] and the importance of these protons has been shown experimentally via selective deuteration.[27,31,32] As the protons that are proximal to the unpaired electron spin are critical to MAS-DNP, it is of great interest to detect them via NMR, at least by indirect means.

In this Letter, we introduce a Nuclear−Nuclear Double Resonance (NUDOR) technique to indirectly detect protons in and around biradicals via detection of remote protons. The experiment is used to analyze the role of those protons close to the radicals in the cross effect DNP mechanism, i.e. how critical they are to the bulk nuclear spin hyperpolarization process. The approach, which uses off-resonance irradiation (Figure 1), produces data analogous to an Electron−Nuclear Double Resonance (ENDOR)[33] experiment. This NUDOR experiment is used to show that in biradicals like TEKPol[34] and AMUPol,[35] the strongly coupled protons in the biradicals play an essential role in MAS-DNP. It also proves that these strongly coupled protons are not critical for the performance of a biradical called AsymPol-TEK.[36] This was further validated by evaluating a series of partially deuterated derivatives, confirming that the protons in AsymPol-TEK biradicals do not significantly contribute to DNP because of strong electron−electron interactions within the molecule.[28] This insight is valuable for designing future biradicals, as it indicates that these protons may not be as critical in certain cases.

Probing otherwise invisible spins, using observable NMR or EPR signals, is well-known in magnetic resonance.[37−39] In EPR, the Electron−Electron Double Resonance (ELDOR) experiment relies on the irradiation of forbidden transitions to observe nuclei in close proximity to the electron spin. In NMR, the widely utilized Chemical Exchange Saturation Transfer

Received: November 11, 2024
Revised: December 20, 2024
Accepted: December 26, 2024
Published: January 9, 2025

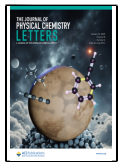

Downloaded via NATL AND UNIV LBRY OF ICELAND on February 17, 2025 at 11:06:51 (UTC).
See https://pubs.acs.org/sharingguidelines for options on how to legitimately share published articles.

ACS Publications © 2025 American Chemical Society

https://doi.org/10.1021/acs.jpclett.4c03254
J. Phys. Chem. Lett. 2025, 16, 635−641

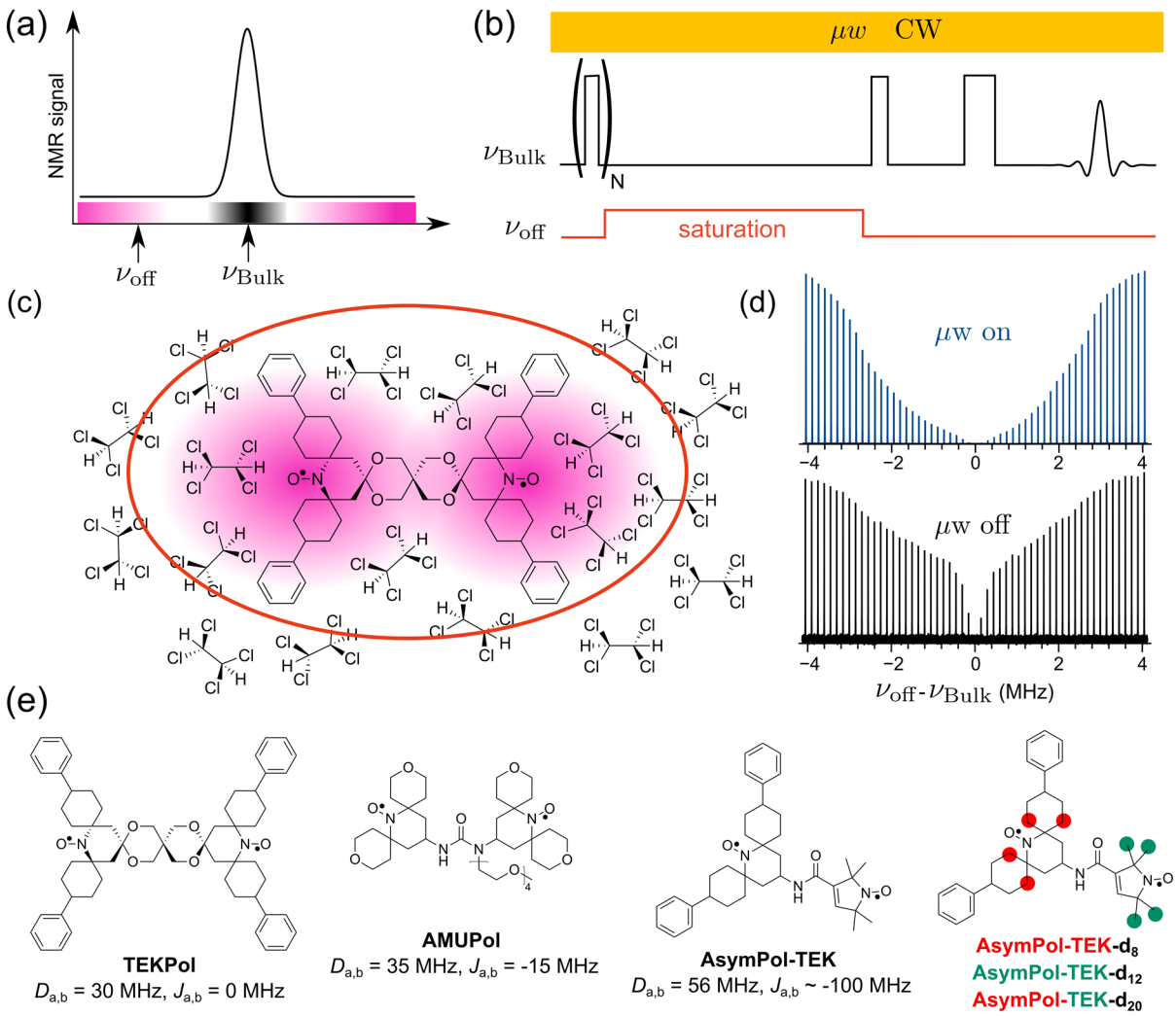

Figure 1. (a) Schematic of a ^{1}H NMR spectrum and position of the on-resonance (ν_{Bulk}) and off-resonance (ν_{off}) radiofrequency (rf) irradiations. (b) Pulse sequence used for NUDOR: the bulk protons are first presaturated and subsequently a long off-resonance saturation pulse (~500 ms, 15 kHz rf) is applied, followed by detection of the bulk protons with an echo sequence. The resulting spectra are collected with and without μw irradiation. (c) Structure of the biradical TEKPol in a frozen 1,1,2,2-tetrachloroethane (TCE) solution. The purple color indicates the radius for hyperfine coupling; the gradient illustrates the strength of the coupling. The oval circle (red) represents the volume of the protons that are saturated by the ν_{off} irradiation. (d) Example of the NUDOR profile for TEKPol with and without μw irradiation. (e) Structures of the biradicals studied using NUDOR in this work.

(CEST)[37] relies on weak radiofrequency (rf) fields to saturate invisible protons, which affects the observable proton spins by chemical exchange. Similarly, one can use the homonuclear spin diffusion instead of the chemical exchange to detect a site of interest. This is used, for example, in Progressive Saturation of the Proton Reservoir (PROSPR).[40] Here, the pulse sequence is dubbed NUDOR in reference to the ELDOR experiment.[41,42]

The idea behind the experiment described here is that if the unobservable, strongly coupled protons (i.e., protons that are strongly hyperfine coupled to the electron spins) in or near the biradical molecules contribute to the DNP mechanism, the signal intensity (I) of the observable bulk proton spin bath, with and without microwave (μw) irradiation (denoted by the DNP enhancement factor, $\epsilon_{on/off} = I_{on}/I_{off}$), can be modulated by perturbing the spin states of the strongly coupled nuclei. This hypothesis would be valid if the strongly coupled protons are essential to the DNP mechanism (*vide infra*). The NMR spectrum of the biradical protons (purple region) span a much higher frequency range than the spectrum of the bulk protons (black region, Figure 1a), due to the strong hyperfine couplings with the unpaired electrons. In NUDOR, the initial pulse train presaturates the bulk proton signal and subsequently, a long and low power saturation pulse (500 ms at a rf nutation of 15 kHz) is applied at a frequency ν_{off}, where ν_{off} is an off-resonance frequency with respect to the observable bulk proton signal. Finally, the signal of the bulk protons is detected using a spin echo sequence at the frequency ν_{Bulk} (Figure 1b). Changing the offset corresponds to changing the radius of a shell surrounding each radical: the protons located within this radius are partially saturated (Figure 1c). Then, spin diffusion transports this saturation to the observable bulk signal. MAS modulates the electron−nuclear hyperfine couplings, which results in a spread of the saturation across a wider frequency range, and also results in more efficient spin diffusion due to nuclear dipolar rotor events.[10,24,43] It is to note that the effect of the pulse sequence

https://doi.org/10.1021/acs.jpclett.4c03254
J. Phys. Chem. Lett. 2025, 16, 635−641

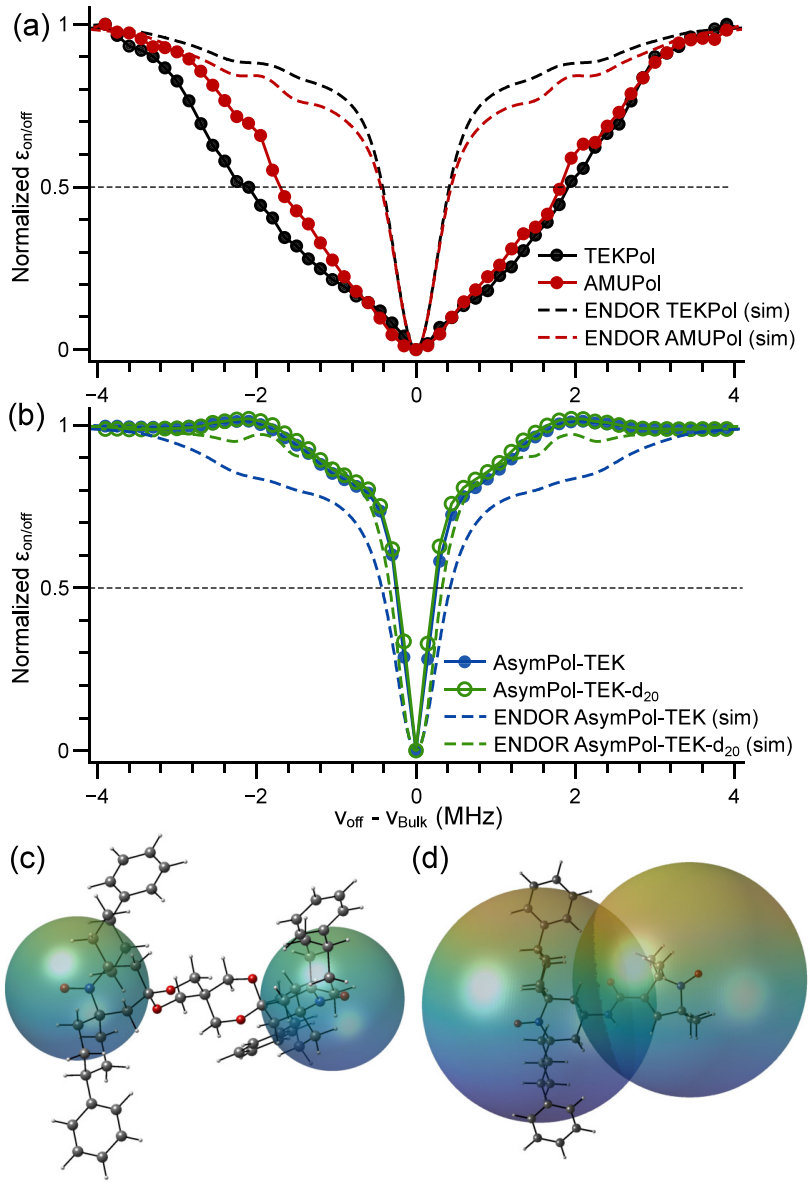

Figure 2. NUDOR profiles of (a) 16 mM TEKPol in TCE (black) and 10 mM AMUPol in glycerol-d_8/D_2O/H_2O (6/4/1 vol %) (red), and (b) 10 mM AsymPol-TEK (blue) and 10 mM AsymPol-TEK-d_{20} (green) in TCE. Dashed lines correspond to simulated ENDOR spectra. (c) Sphere of 0.35 nm around the NO• group of TEKPol, corresponding to $|\nu_{off}^{50\%} - \nu_{Bulk}| \approx 0.2$ MHz. (d) Sphere of 0.7 nm around the NO• group of AsymPol-TEK corresponding to $|\nu_{off}^{50\%} - \nu_{Bulk}| \approx 0.2$ MHz.

can be easily reproduced with standard spin dynamics simulations on a three-spin system (see Figure S5).

A series of 1D ^{1}H solid-state NMR spectra can be obtained at ν_{Bulk} by varying ν_{off}. The experiments are performed in the presence and absence of μw irradiation to probe the involvement of the protons in the DNP mechanism. Taking the ratios of the μw on and off signal intensities also limits the distortion of the profile due to the rf properties of the NMR probe (see SI). An example of the effect of the variable off-resonance irradiation is shown in Figure 1d for the biradical TEKPol (Figure 1e), both in the presence and absence of μw irradiation. In both cases, the off-resonance irradiation impacts the bulk NMR signal intensity up to $|\nu_{off} - \nu_{Bulk}| \approx 4$ MHz. The proposed NUDOR experiment is also analogous to the SPIDEST experiment[44] but uses continuous-wave irradiation combined with the DNP enhancement factors to obtain the "hyperfine-shifted" spectra.[44]

Figure 2a shows the NUDOR profile, i.e. the normalized DNP enhancement factor plotted as a function of ν_{off}, for AMUPol in glycerol-d_8/D_2O/H_2O (6/4/1 vol %) and TEKPol in 1,1,2,2-tetrachloroethane (TCE). The profiles are normalized with respect to the reference DNP enhancement factor obtained in the absence of the saturation pulse. As expected, the enhancement is null when $\nu_{off} = \nu_{Bulk}$ since the on-resonance saturation nullifies the bulk signal. As the irradiation frequency of the saturation pulse is shifted away from the bulk resonance, the enhancement increases. Once the off-resonance saturation pulse is applied beyond 4 MHz, the observed NUDOR enhancement is equal to the reference DNP enhancement factor, i.e. when obtained without the saturation pulse. The calculated ENDOR spectra of the biradicals were obtained with EasySpin[45,46] using the hyperfine couplings calculated via DFT (see SI). In the case of AMUPol and TEKPol, the total widths of the experimental NUDOR profiles

https://doi.org/10.1021/acs.jpclett.4c03254
J. Phys. Chem. Lett. 2025, 16, 635−641

and calculated ENDOR spectra correlate well (Figure 2a). Interestingly, the NUDOR profiles show features that are present in the theoretical ENDOR spectra (Figure 2a). For example, the shoulders near +2 and −2 MHz in the NUDOR profiles of both TEKPol and AMUPol are reproduced in the calculated ENDOR spectra. Note that a better match between NUDOR and ENDOR for AMUPol can be obtained by using lower power saturation pulses (10 kHz rf, see Figure S3a)—this comparison confirms that the NUDOR experiment indeed senses the nuclei in the vicinity of the biradical.

For AMUPol and TEKPol, the NUDOR experiments show that 50% of the enhancement is recovered at $|\nu_{\mathrm{off}}^{50\%} - \nu_{\mathrm{Bulk}}| \approx 2$ MHz; such large 2 MHz hyperfine couplings correspond to protons located proximate to the nitroxide (NO•) group (located within ca. 0.35 nm; the corresponding spheres are shown in Figure 2c). Since TEKPol and AMUPol have modest electron−electron couplings,[47] they may be inefficient at *directly* hyperpolarizing the bulk medium.[16,27,28] Indeed, the rate at which the CE polarizes the nuclei (R_{CE}) can be approximated as

$$R_{\mathrm{CE}} \propto \left(\frac{\langle (D_{a,b} + 2J_{a,b})^2 \rangle \langle (A_{a,n}^{\pm} - A_{b,n}^{\pm})^2 \rangle}{\omega_n^2} \right) \tag{1}$$

where $D_{a,b}$ and $J_{a,b}$ are the electron−electron dipolar coupling and the exchange interaction, respectively. $A_{a,n}^{\pm}$ and $A_{b,n}^{\pm}$ are the pseudosecular hyperfine coupling to the nucleus n and ω_n is the nuclear Larmor frequency.[16,28] This relation shows that for a moderate $\langle (D_{a,b}+2J_{a,b})^2 \rangle$, stronger $\langle (A_{a,n}^{\pm}-A_{b,n}^{\pm})^2 \rangle$ is required for efficient polarization. The NUDOR experiments thus confirm that the protons in the biradicals AMUPol and TEKPol are critical for the hyperpolarization transfer. This result is entirely consistent with the previous experimental observations with TEKPol.[27]

On the other hand, we have previously used deuterated AsymPol biradicals and extensive large spin-system simulations to show that the protons in the AsymPol biradicals play a limited role in polarization transfer.[16,28] To experimentally confirm this notion, the NUDOR experiment was applied to two biradicals in the AsymPol family: AsymPol-TEK[36] and AsymPol-TEK-d_{20}, which has been newly synthesized and reported here (Figure 1d). These radicals are identical, except that the protons with the largest hyperfine couplings have been replaced with deuterons in AsymPol-TEK-d_{20} (for synthesis, see SI). The results are striking: the NUDOR profiles of both biradicals are identical, showing that the protons that were replaced by deuterons do not participate in the DNP mechanism (Figure 2b). In both cases, a narrow component close to the bulk resonance frequency is observed, and at further off-resonance frequencies, the enhancement recovers sharply back to the reference value. The NUDOR profiles of AsymPol-TEK and AsymPol-TEK-d_{20} are identical, which is different from the expected ENDOR spectra. Indeed, according to the ENDOR simulations, the two biradicals should have strikingly different ENDOR spectra and thus different NUDOR profiles (dotted lines Figure 2b). In particular, the predicted ENDOR spectrum of AsymPol-TEK shows signals in the region ranging from 1.5 to 3 MHz. However, these features are not observed in the experimental NUDOR profiles, which demonstrates that saturating or removing a few of the most strongly coupled nuclear spins in AsymPol-TEK (i.e., the protons closest to the nitroxide moieties), does not affect the CE DNP process. This means that the protons that contributes most to the hyperpolarization of the bulk are located outside the biradical molecule, i.e. in the solvent, similar to our previous observation with AsymPol derivatives.[28]

An intriguing observation for AsymPol-TEK is that at $|\nu_{\mathrm{off}} - \nu_{\mathrm{Bulk}}| \approx 2$ MHz, there is a reproducible overshoot of the enhancement by ∼1−2%. Note that the actual signal intensity did not increase with respect to the reference experiment without saturation (see Figure S2). Rationalizing this minor observation is beyond the scope of this work.

In the case of AsymPol-TEK, 50% of the enhancement is recovered at $|\nu_{\mathrm{off}}^{50\%} - \nu_{\mathrm{Bulk}}| \approx 0.2$ MHz, corresponding to a factor ∼10 smaller than with AMUPol or TEKPol. This value agrees with the ratio of electron−electron spin couplings:[25,28,48]

$$\frac{\langle (D_{a,b} + 2J_{a,b})^2 \rangle_{\mathrm{AsymPol-TEK}}}{\langle (D_{a,b} + 2J_{a,b})^2 \rangle_{\mathrm{TEKPol}}} \approx 20 \tag{2}$$

$$\frac{\langle (D_{a,b} + 2J_{a,b})^2 \rangle_{\mathrm{AsymPol-TEK}}}{\langle (D_{a,b} + 2J_{a,b})^2 \rangle_{\mathrm{AMUPol}}} \approx 10 \tag{3}$$

A hyperfine coupling value of 0.2 MHz corresponds to protons located at ∼0.7 nm, i.e., relatively far from the NO• as depicted in Figure 2d. Thus, for AsymPol-TEK, only protons that are not in the vicinity of the nitroxide (i.e., those that are either far on the backbone or in the solvent), are essential for DNP. To further confirm this observation, selectively deuterated derivatives AsymPol-TEK-d_8 and AsymPol-TEK-d_{12} were synthesized (see SI), in addition to the aforementioned AsymPol-TEK-d_{20} (Figure 1e), in which the protons with the strongest hyperfine couplings are removed. The DNP enhancement and characteristic DNP buildup time (T_B) for these compounds are shown in Figure 3a and b, respectively.

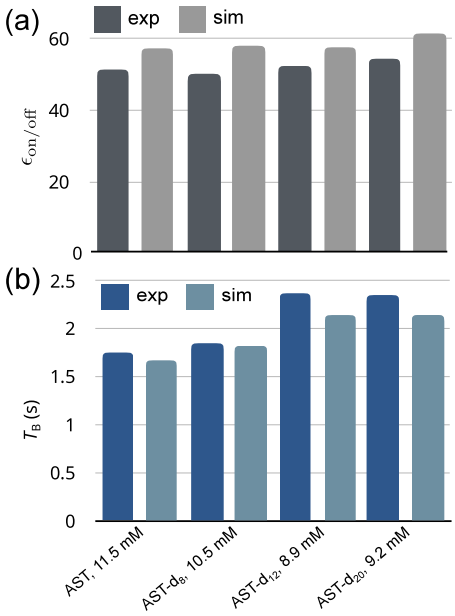

Figure 3. Evolution of (a) DNP enhancements and (b) build-up time as a function of deuteration level in AsymPol-TEK. In (a), experiments and simulations are shown in dark and light gray, respectively, and in (b) experiments and simulations are shown in dark and light blue, respectively.

https://doi.org/10.1021/acs.jpclett.4c03254
J. Phys. Chem. Lett. 2025, 16, 635−641

The enhancements are similar for all isotopologues and fall in the range between 50 and 58. Some variation is observed in the buildup times, ranging from 1.6 to 2.3 s. The fact that the enhancements are similar, supports the idea that the strongly coupled protons do not play an essential role in the DNP. This is in stark contrast to TEKPol, where smaller enhancements were obtained upon deuteration.[27,28] It should be noted that the variations in the build-up times, which may appear at first to follow the previous trends observed by Venkatesh *et al.* of increased build-up times with more deuteration,[27] was found to be due to slightly lower concentrations of the deuterated samples.

The AsymPol-TEKs should have the same geometry/magnetic parameters as previously reported,[36] because their liquid state EPR spectra are identical (Figure S4). Accounting for the differences in concentration of the biradicals, it is possible to perform quantitative quantum simulations. Using large spin system simulations[24,25,29] and DFT/Molecular Dynamics[25,29] as input parameters for the hyperfine couplings on the biradicals, both the enhancements and buildup time are very well reproduced (Figure 3). As the MAS-DNP simulations are quantitatively accurate, we used them to check the impact of deuteration, assuming identical biradical concentration. The results (Figure S7) indicate that identical buildup should indeed be expected for all deuteration levels. As such, this confirms the outcome of previous work[16,28] and of the NUDOR experiments: under a magnetic field of 14.1 T, AsymPol-TEK predominantly hyperpolarizes the protons of the solvent directly, and that the relayed hyperpolarization through the protons in the biradicals is less favorable.

In summary, we have shown that NUDOR can be used to detect strongly coupled protons in nitroxide biradicals. This experiment allows identification of the protons that most contribute to for the hyperpolarization of the bulk nuclei. At 14.1 T, it provides a definite and direct proof that the protons in the biradicals of TEKPol and AMUPol contribute to the DNP under MAS, while the protons in the AsymPols play a minor role, as previously proposed.[28] We anticipate that the NUDOR profiles for a given biradical may depend on the experimental conditions, such as the magnetic field and the MAS frequency, as well as the length and rf power of the saturation pulse. For example, $|\nu_{\mathrm{off}}^{(50\%)}|$ should increase for faster MAS experiments based on previous simulations.[26] At higher magnetic field is likely that the $|\nu_{\mathrm{off}}^{(50\%)}|$ of AsymPol-TEK will increase at as R_{CE} diminishes, meaning that protons in the biradical may play a greater role. Reciprocally, the $|\nu_{\mathrm{off}}^{(50\%)}|$ should decrease for AMUPol and TEKPol as the field is lowered. The NUDOR experiment thus provides a simple way to tune the properties of a given biradical for a set of experimental conditions. Finally, in cases where nuclear spins close to the polarizing agent are critical to the DNP mechanism (for example TEKPol/AMUPol), the NUDOR and ENDOR profiles appear to share similar features. It may thus be possible to apply the method to other polarizing agents, such as monoradicals[49,50] metal ions,[51,52] or other species[53−55] to determine, at least partially, the corresponding ENDOR spectra of nuclear spins that are very close to the electron, without the need of an EPR instrument.

■ ASSOCIATED CONTENT

Supporting Information

The Supporting Information is available free of charge at https://pubs.acs.org/doi/10.1021/acs.jpclett.4c03254.

Experimental details and derivation of the equations (PDF)

■ AUTHOR INFORMATION

Corresponding Author

Frédéric Mentink-Vigier − *National High Magnetic Field Laboratory, Florida State University, Tallahassee, Florida 32310, United States; Department of Chemistry and Biochemistry, Florida State University, Tallahassee, Florida 32306, United States;* orcid.org/0000-0002-3570-9787; Email: fmentink@fsu.edu

Authors

Satyaki Chatterjee − *Department of Chemistry, Science Institute, University of Iceland, 107 Reykjavik, Iceland;* orcid.org/0000-0003-3543-7758

Faith J. Scott − *National High Magnetic Field Laboratory, Florida State University, Tallahassee, Florida 32310, United States;* orcid.org/0000-0003-3903-8842

Snorri Th. Sigurdsson − *Department of Chemistry, Science Institute, University of Iceland, 107 Reykjavik, Iceland;* orcid.org/0000-0003-2492-1456

Amrit Venkatesh − *National High Magnetic Field Laboratory, Florida State University, Tallahassee, Florida 32310, United States;* orcid.org/0000-0001-5319-9269

Complete contact information is available at: https://pubs.acs.org/10.1021/acs.jpclett.4c03254

Notes

The authors declare no competing financial interest.

■ ACKNOWLEDGMENTS

The National High Magnetic Field Laboratory (NHMFL) is funded by the National Science Foundation Division of Materials Research (DMR-2128556) and the State of Florida. A portion of this work was supported by National Institutes of Health Grant RM1-GM148766. This project has received partial support from the European Union's Horizon 2020 research and innovation programme under Grant Agreement 101008500 (PANACEA). F.J.S. acknowledges support from a Postdoctoral Scholar Award from the Provost's Office at Florida State University. This work was also supported by the Icelandic Research Fund (Grant 239662), the University of Iceland Research Fund (S.Th.S.), and a doctoral fellowship from the University of Iceland Research Fund (S.C.).

■ REFERENCES

(1) Reif, B.; Ashbrook, S. E.; Emsley, L.; Hong, M. Solid-State NMR Spectroscopy. *Nat. Rev. Methods Primer* **2021**, *1* (1), 1−23.

(2) Lilly Thankamony, A. S.; Wittmann, J. J.; Kaushik, M.; Corzilius, B. Dynamic Nuclear Polarization for Sensitivity Enhancement in Modern Solid-State NMR. *Prog. Nucl. Magn. Reson. Spectrosc.* **2017**, *102−103*, 120−195.

(3) Lee, D.; Hediger, S.; De Paëpe, G. Is Solid-State NMR Enhanced by Dynamic Nuclear Polarization? *Solid State Nucl. Magn. Reson.* **2015**, *66−67*, 6−20.

(4) Rankin, A. G. M.; Trébosc, J.; Pourpoint, F.; Amoureux, J.-P.; Lafon, O. Recent Developments in MAS DNP-NMR of Materials. *Solid State Nucl. Magn. Reson.* **2019**, *101*, 116−143.

(5) Chow, W. Y.; De Paëpe, G.; Hediger, S. Biomolecular and Biological Applications of Solid-State NMR with Dynamic Nuclear Polarization Enhancement. *Chem. Rev.* **2022**, *122* (10), 9795−9847.

(6) Ghassemi, N.; Poulhazan, A.; Deligey, F.; Mentink-Vigier, F.; Marcotte, I.; Wang, T. Solid-State NMR Investigations of

Extracellular Matrixes and Cell Walls of Algae, Bacteria, Fungi, and Plants. *Chem. Rev.* **2022**, *122* (10), 10036−10086.
(7) Rossini, A. J.; Zagdoun, A.; Lelli, M.; Lesage, A.; Copéret, C.; Emsley, L. Dynamic Nuclear Polarization Surface Enhanced NMR Spectroscopy. *Acc. Chem. Res.* **2013**, *46* (9), 1942−1951.
(8) Ni, Q. Z.; Daviso, E.; Can, T. V.; Markhasin, E.; Jawla, S. K.; Swager, T. M.; Temkin, R. J.; Herzfeld, J.; Griffin, R. G. High Frequency Dynamic Nuclear Polarization. *Acc. Chem. Res.* **2013**, *46* (9), 1933−1941.
(9) Casano, G.; Karoui, H.; Ouari, O. Evolution and Outlook in Free Radical Development for DNP. In *eMagRes*; John Wiley & Sons: Chichester, UK, 2018; Vol. 7, pp 195−208. .
(10) Kundu, K.; Mentink-Vigier, F.; Feintuch, A.; Vega, S. DNP Mechanisms. In *eMagRes*; John Wiley & Sons: Chichester, UK, 2019; pp 295−338. .
(11) Thurber, K. R.; Tycko, R. Theory for Cross Effect Dynamic Nuclear Polarization under Magic-Angle Spinning in Solid State Nuclear Magnetic Resonance: The Importance of Level Crossings. *J. Chem. Phys.* **2012**, *137* (8), 084508.
(12) Mentink-Vigier, F.; Akbey, Ü.; Hovav, Y.; Vega, S.; Oschkinat, H.; Feintuch, A. Fast Passage Dynamic Nuclear Polarization on Rotating Solids. *J. Magn. Reson.* **2012**, *224*, 13−21.
(13) Thurber, K. R.; Tycko, R. Perturbation of Nuclear Spin Polarizations in Solid State NMR of Nitroxide-Doped Samples by Magic-Angle Spinning without Microwaves. *J. Chem. Phys.* **2014**, *140* (18), 184201.
(14) Mentink-Vigier, F.; Paul, S.; Lee, D.; Feintuch, A.; Hediger, S.; Vega, S.; De Paëpe, G. Nuclear Depolarization and Absolute Sensitivity in Magic-Angle Spinning Cross Effect Dynamic Nuclear Polarization. *Phys. Chem. Chem. Phys.* **2015**, *17* (34), 21824−21836.
(15) Mentink-Vigier, F.; Marin-Montesinos, I.; Jagtap, A. P.; Halbritter, T.; van Tol, J.; Hediger, S.; Lee, D.; Sigurdsson, S. Th.; De Paëpe, G. Computationally Assisted Design of Polarizing Agents for Dynamic Nuclear Polarization Enhanced NMR: The AsymPol Family. *J. Am. Chem. Soc.* **2018**, *140* (35), 11013−11019.
(16) Scott, F. J.; Eddy, S.; Gullion, T.; Mentink-Vigier, F. Sorbitol-Based Glass Matrices Enable Dynamic Nuclear Polarization beyond 200 K. *J. Phys. Chem. Lett.* **2024**, *15*, 8743−8751.
(17) Equbal, A.; Tagami, K.; Han, S. Balancing Dipolar and Exchange Coupling in Biradicals to Maximize Cross Effect Dynamic Nuclear Polarization. *Phys. Chem. Chem. Phys.* **2020**, *22* (24), 13569−13579.
(18) Equbal, A.; Leavesley, A.; Jain, S. K.; Han, S. Cross-Effect Dynamic Nuclear Polarization Explained: Polarization, Depolarization, and Oversaturation. *J. Phys. Chem. Lett.* **2019**, *10* (3), 548−558.
(19) Tan, K. O.; Mardini, M.; Yang, C.; Ardenkjær-Larsen, J. H.; Griffin, R. G. Three-Spin Solid Effect and the Spin Diffusion Barrier in Amorphous Solids. *Sci. Adv.* **2019**, *5* (7), No. eaax2743.
(20) Stern, Q.; Cousin, S. F.; Mentink-Vigier, F.; Pinon, A. C.; Elliott, S. J.; Cala, O.; Jannin, S. Direct Observation of Hyperpolarization Breaking through the Spin Diffusion Barrier. *Sci. Adv.* **2021**, *7* (18), No. eabf5735.
(21) Wolfe, J. P. Direct Observation of a Nuclear Spin Diffusion Barrier. *Phys. Rev. Lett.* **1973**, *31* (15), 907−910.
(22) Wittmann, J. J.; Eckardt, M.; Harneit, W.; Corzilius, B. Electron-Driven Spin Diffusion Supports Crossing the Diffusion Barrier in MAS DNP. *Phys. Chem. Chem. Phys.* **2018**, *20* (16), 11418−11429.
(23) Karabanov, A.; Wiśniewski, D.; Lesanovsky, I.; Köckenberger, W. Dynamic Nuclear Polarization as Kinetically Constrained Diffusion. *Phys. Rev. Lett.* **2015**, *115* (2), 020404.
(24) Mentink-Vigier, F.; Vega, S.; De Paëpe, G. Fast and Accurate MAS-DNP Simulations of Large Spin Ensembles. *Phys. Chem. Chem. Phys.* **2017**, *19* (5), 3506−3522.
(25) Mentink-Vigier, F.; Dubroca, T.; Van Tol, J.; Sigurdsson, S. Th. The Distance between G-Tensors of Nitroxide Biradicals Governs MAS-DNP Performance: The Case of the bTurea Family. *J. Magn. Reson.* **2021**, *329*, 107026.
(26) Perras, F. A.; Raju, M.; Carnahan, S. L.; Akbarian, D.; Van Duin, A. C. T.; Rossini, A. J.; Pruski, M. Full-Scale Ab Initio Simulation of Magic-Angle-Spinning Dynamic Nuclear Polarization. *J. Phys. Chem. Lett.* **2020**, *11* (14), 5655−5660.
(27) Venkatesh, A.; Casano, G.; Rao, Y.; De Biasi, F.; Perras, F. A.; Kubicki, D. J.; Siri, D.; Abel, S.; Karoui, H.; Yulikov, M.; Ouari, O.; Emsley, L. Deuterated TEKPol Biradicals and the Spin-Diffusion Barrier in MAS DNP. *Angew. Chem., Int. Ed.* **2023**, *62* (31), No. e202304844.
(28) Chatterjee, S.; Venkatesh, A.; Sigurdsson, S. Th.; Mentink-Vigier, F. Role of Protons in and around Strongly Coupled Nitroxide Biradicals for Cross-Effect Dynamic Nuclear Polarization. *J. Phys. Chem. Lett.* **2024**, *15* (8), 2160−2168.
(29) Harrabi, R.; Halbritter, T.; Aussenac, F.; Dakhlaoui, O.; van Tol, J.; Damodaran, K. K.; Lee, D.; Paul, S.; Hediger, S.; Mentink-Vigier, F.; Sigurdsson, S. Th.; De Paëpe, G. Highly Efficient Polarizing Agents for MAS-DNP of Proton-Dense Molecular Solids. *Angew. Chem., Int. Ed.* **2022**, *61* (12), No. e202114103.
(30) Perras, F. A.; Carnahan, S. L.; Lo, W.-S.; Ward, C. J.; Yu, J.; Huang, W.; Rossini, A. J. Hybrid Quantum-Classical Simulations of Magic Angle Spinning Dynamic Nuclear Polarization in Very Large Spin Systems. *J. Chem. Phys.* **2022**, *156* (12), 124112.
(31) Perras, F. A.; Reinig, R. R.; Slowing, I. I.; Sadow, A. D.; Pruski, M. Effects of Biradical Deuteration on the Performance of DNP: Towards Better Performing Polarizing Agents. *Phys. Chem. Chem. Phys.* **2016**, *18* (1), 65−69.
(32) Geiger, M.-A.; Orwick-Rydmark, M.; Märker, K.; Franks, W. T.; Akhmetzyanov, D.; Stöppler, D.; Zinke, M.; Specker, E.; Nazaré, M.; Diehl, A.; van Rossum, B.-J.; Aussenac, F.; Prisner, T.; Akbey, Ü.; Oschkinat, H. Temperature Dependence of Cross-Effect Dynamic Nuclear Polarization in Rotating Solids: Advantages of Elevated Temperatures. *Phys. Chem. Chem. Phys.* **2016**, *18* (44), 30696−30704.
(33) Feher, G. Observation of Nuclear Magnetic Resonances via the Electron Spin Resonance Line. *Phys. Rev.* **1956**, *103* (3), 834−835.
(34) Zagdoun, A.; Casano, G.; Ouari, O.; Schwarzwälder, M.; Rossini, A. J.; Aussenac, F.; Yulikov, M.; Jeschke, G.; Copéret, C.; Lesage, A.; Tordo, P.; Emsley, L. Large Molecular Weight Nitroxide Biradicals Providing Efficient Dynamic Nuclear Polarization at Temperatures up to 200 K. *J. Am. Chem. Soc.* **2013**, *135* (34), 12790−12797.
(35) Sauvée, C.; Rosay, M.; Casano, G.; Aussenac, F.; Weber, R. T.; Ouari, O.; Tordo, P. Highly Efficient, Water-Soluble Polarizing Agents for Dynamic Nuclear Polarization at High Frequency. *Angew. Chem., Int. Ed.* **2013**, *52* (41), 10858−10861.
(36) Harrabi, R.; Halbritter, T.; Alarab, S.; Chatterjee, S.; Wolska-Pietkiewicz, M.; Damodaran, K. K.; Van Tol, J.; Lee, D.; Paul, S.; Hediger, S.; Sigurdsson, S. Th.; Mentink-Vigier, F.; De Paëpe, G. AsymPol-TEKs as Efficient Polarizing Agents for MAS-DNP in Glass Matrices of Non-Aqueous Solvents. *Phys. Chem. Chem. Phys.* **2024**, *26* (6), 5669−5682.
(37) Ward, K. M.; Aletras, A. H.; Balaban, R. S. A New Class of Contrast Agents for MRI Based on Proton Chemical Exchange Dependent Saturation Transfer (CEST). *J. Magn. Reson.* **2000**, *143* (1), 79−87.
(38) Fawzi, N. L.; Ying, J.; Ghirlando, R.; Torchia, D. A.; Clore, G. M. Atomic-Resolution Dynamics on the Surface of Amyloid-β Protofibrils Probed by Solution NMR. *Nature* **2011**, *480* (7376), 268−272.
(39) Long, D.; Bouvignies, G.; Kay, L. E. Measuring Hydrogen Exchange Rates in Invisible Protein Excited States. *Proc. Natl. Acad. Sci. U. S. A.* **2014**, *111* (24), 8820−8825.
(40) Jaroszewicz, M. J.; Altenhof, A. R.; Schurko, R. W.; Frydman, L. Sensitivity Enhancement by Progressive Saturation of the Proton Reservoir: A Solid-State NMR Analogue of Chemical Exchange Saturation Transfer. *J. Am. Chem. Soc.* **2021**, *143* (47), 19778−19784.
(41) Hyde, J. S.; Chien, J. C. W.; Freed, J. H. Electron-Electron Double Resonance of Free Radicals in Solution. *J. Chem. Phys.* **1968**, *48* (9), 4211−4226.

(42) Goldfarb, D.; Harris, R. K.; Wasylishen, R. L. ELDOR-Detected NMR. In *eMagRes*; John Wiley & Sons: Chichester, UK, 2017; pp 101−114. .

(43) Mentink-Vigier, F.; Akbey, Ü.; Oschkinat, H.; Vega, S.; Feintuch, A. Theoretical Aspects of Magic Angle Spinning - Dynamic Nuclear Polarization. *J. Magn. Reson.* **2015**, *258*, 102−120.

(44) Pang, Z.; Sheberstov, K.; Rodin, B. A.; Lumsden, J.; Banerjee, U.; Abergel, D.; Mentink-Vigier, F.; Bodenhausen, G.; Tan, K. O. Hypershifted Spin Spectroscopy with Dynamic Nuclear Polarization at 1.4 K. *Sci. Adv.* **2024**, *10* (50), No. eadr7160.

(45) Stoll, S.; Schweiger, A. EasySpin, a Comprehensive Software Package for Spectral Simulation and Analysis in EPR. *J. Magn. Reson.* **2006**, *178* (1), 42−55.

(46) Stoll, S. CW-EPR Spectral Simulations. In *Methods in Enzymology*; Elsevier, 2015; Vol. *563*, pp 121−142. DOI: 10.1016/bs.mie.2015.06.003.

(47) Mentink-Vigier, F.; Barra, A.-L.; van Tol, J.; Hediger, S.; Lee, D.; De Paëpe, G. *De Novo* Prediction of Cross-Effect Efficiency for Magic Angle Spinning Dynamic Nuclear Polarization. *Phys. Chem. Chem. Phys.* **2019**, *21* (4), 2166−2176.

(48) Soetbeer, J.; Gast, P.; Walish, J. J.; Zhao, Y.; George, C.; Yang, C.; Swager, T. M.; Griffin, R. G.; Mathies, G. Conformation of Bis-Nitroxide Polarizing Agents by Multi-Frequency EPR Spectroscopy. *Phys. Chem. Chem. Phys.* **2018**, *20* (39), 25506−25517.

(49) Can, T. V.; Caporini, M. A.; Mentink-Vigier, F.; Corzilius, B.; Walish, J. J.; Rosay, M.; Maas, W. E.; Baldus, M.; Vega, S.; Swager, T. M.; Griffin, R. G. Overhauser Effects in Insulating Solids. *J. Chem. Phys.* **2014**, *141* (6), 064202.

(50) Ji, X.; Can, T. V.; Mentink-Vigier, F.; Bornet, A.; Milani, J.; Vuichoud, B.; Caporini, M. A.; Griffin, R. G.; Jannin, S.; Goldman, M.; Bodenhausen, G. Overhauser Effects in Non-Conducting Solids at 1.2 K. *J. Magn. Reson.* **2018**, *286*, 138−142.

(51) Jardón-Álvarez, D.; Leskes, M. Metal Ions Based Dynamic Nuclear Polarization: MI-DNP. *Prog. Nucl. Magn. Reson. Spectrosc.* **2023**, *138−139*, 70−104.

(52) Hope, M. A.; Björgvinsdóttir, S.; Halat, D. M.; Menzildjian, G.; Wang, Z.; Zhang, B.; MacManus-Driscoll, J. L.; Lesage, A.; Lelli, M.; Emsley, L.; Grey, C. P. Endogenous ^{17}O Dynamic Nuclear Polarization of Gd-Doped CeO_2 from 100 to 370 K. *J. Phys. Chem. C* **2021**, *125* (34), 18799−18809.

(53) Carnahan, S. L.; Chen, Y.; Wishart, J. F.; Lubach, J. W.; Rossini, A. J. Magic Angle Spinning Dynamic Nuclear Polarization Solid-State NMR Spectroscopy of γ-Irradiated Molecular Organic Solids. *Solid State Nucl. Magn. Reson.* **2022**, *119*, 101785.

(54) Miao, Z.; Scott, F. J.; van Tol, J.; Bowers, C. R.; Veige, A. S.; Mentink-Vigier, F. Soliton Based Dynamic Nuclear Polarization: An Overhauser Effect in Cyclic Polyacetylene at High Field and Room Temperature. *J. Phys. Chem. Lett.* **2024**, *15*, 3369−3375.

(55) Hope, M. A.; Rinkel, B. L. D.; Gunnarsdóttir, A. B.; Märker, K.; Menkin, S.; Paul, S.; Sergeyev, I. V.; Grey, C. P. Selective NMR Observation of the SEI-Metal Interface by Dynamic Nuclear Polarisation from Lithium Metal. *Nat. Commun.* **2020**, *11* (1), 2224.

https://doi.org/10.1021/acs.jpclett.4c03254
J. Phys. Chem. Lett. 2025, 16, 635−641